

**FEDSM2002-31235**

**THIN LIQUID FILM FLOW ON A ROTATING ANNULAR DISK: ASYMPTOTIC SOLUTION**

**Prabir Daripa**

Department of Mathematics  
 Texas A&M University, College Station, TX-77843  
 Email: daripa@math.tamu.edu

**B. S. Dandapat  
 P. C. Ray**

Physics and Applied Mathematics Unit  
 ISI, Calcutta-700035, India

**ABSTRACT**

We consider the axisymmetric flow of a Newtonian fluid associated with the spreading of a thin liquid film on a rotating annular disk. The effects of surface tension and gravity terms are included. The asymptotic solution for the free surface of the thin film is found using an expansion for the film thickness in powers of a small parameter characterizing the thickness of the film and applying the method of matched asymptotic expansion. This solution can be used to calculate the thickness of the film, the velocity field, and the pressure at any point on the disk with good accuracy. Numerical results are presented for a specific initial distribution of the film thickness. Many features of the spin-coating thinning process are captured by our asymptotic solution. We also produce results which are in excellent agreement with the experimental findings of Daughton and Givens (6) and Hwang and Ma (9).

Keywords: Thin films, asymptotics, rotating disk, surface tension.

**NOMENCLATURE**

$F$  = An arbitrary dependent variable  
 $F_0$  = leading order term in the expansion of  $F$   
 $F_1$  = first order term in the expansion of  $F$   
 $Fr$  = Froude number,  $\sqrt{(\Omega^4 R_0^2 H_0^3 / g \nu^2)}$   
 $H_0$  = maximum value of the initial film thickness  
 $R$  = outer radius of the annular disk  
 $R_0$  = inner radius of the annular disk  
 $Re$  = Reynolds number,  $U_0 H_0 / \nu$

$Q_0$  = amount of liquid deposited initially  
 $\bar{Q}$  = amount of liquid depleted  
 $U_0$  = velocity scale,  $R_0 / t_c$   
 $We$  = Weber number,  $\sigma_0 / R_0 H_0^2 \Omega^2 \rho$   
 $c$  = a constant of integration  
 $c_0$  = constant of integration  
 $c_1$  = constant of integration  
 $c_2$  = constant of integration  
 $g$  = gravity  
 $h$  = non-dimensional film thickness distribution  
 $h_0$  = leading order term in the expansion of  $h$   
 $h_1$  = first order term in the expansion of  $h$   
 $h^c$  = composite film thickness  
 $p$  = non-dimensional pressure  
 $p'$  = pressure  
 $r$  = non-dimensional  $r$ -axis coordinate  
 $r'$  =  $r$ -axis coordinate  
 $t'$  = time  
 $t_c$  = Characteristic time scale,  $\nu / (\Omega H_0)^2$   
 $u$  = non-dimensional speed along  $r$ -axis  
 $u'$  = speed along  $r$ -axis  
 $v$  = non-dimensional azimuthal speed  
 $v'$  = azimuthal speed  
 $w$  = non-dimensional speed along  $z$ -axis  
 $w'$  = speed along  $z$ -axis  
 $z$  = non-dimensional  $z$ -axis coordinate  
 $z'$  =  $z$ -axis coordinate  
**Greek Symbols**  
 $\delta$  = non-dimensional initial film thickness distribution

$\hat{\delta}$  = initial film thickness distribution  
 $\varepsilon$  = small parameter,  $H_0/R_0$   
 $\mu_g$  = viscosity of the gas phase  
 $\mu_l$  = viscosity of the liquid phase  
 $\nu$  = kinematic viscosity of the fluid  
 $\rho$  = density of the liquid  
 $\sigma_0$  = surface tension coefficient  
 $\tau$  = non-dimensional time  
 $\tau_b$  = wave breaking time  
 $\theta$  = polar angle  
 $\Omega$  = uniform angular velocity of the disk

#### Superscripts

$c$  = composite  
 $'$  = dimensional

#### Subscripts

$b$  = break  
 $c$  = characteristic  
 $l$  = liquid  
 $g$  = gas  
 $r$  = first derivative with respect to  $r$   
 $rr$  = second derivative with respect to  $r$   
 $z$  = first derivative with respect to  $z$   
 $zz$  = second derivative with respect to  $z$   
 $0, 1$  = index for the perturbation terms unless specified otherwise  
 $\tau$  = first derivative with respect to  $\tau$

## 1 INTRODUCTION

Production of thin films on solid surfaces has enormous practical applications. Thin liquid films can be produced on smooth solid surfaces either by the action of gravity on stationary vertical/inclined planes or by the action of centrifugal force on rotating disks. The pioneering work of Kapitza (11) on thin viscous fluid layers has been a catalyst for extensive research on the production of thin liquid films under gravity. However, similar studies under centrifugal force, instead of gravity, have received much less attention, in spite of the fact that the centrifugal force can be controlled at any desired level in a proper laboratory setting.

Importance of thin film production on a rotating disk has gained significant momentum over last two decades in connection with the coating on IC chips and other substrates in microelectronics industry. The first theoretical study of the associated viscous flow in this field was carried out by Emslie et al. (7) almost forty years ago. They considered axisymmetric flow of a Newtonian fluid on a planar substrate rotating with constant angular velocity and assumed that a steady state will reach when centrifugal and viscous forces balance each other. A study of this simplified problem allowed the authors to show that the uniformity of the film is not disturbed as the film thins gradually. Subsequent authors have extended this work to include various phys-

ical factors including surface tension, air-shear, non-Newtonian fluids, non-planar substrate, evaporation and adsorption. In this connection, the review article of Larson and Rehg (13) should also be cited.

Over the past three decades, various authors have attempted to explain and understand the various relations among different factors involved in spin-coating process. Daughton and Givens (6) performed careful experiments and showed that the final film thickness is largely insensitive to the initial amount of fluid deposited on the disk, the rate of removal of the fluid, the rotational acceleration and even the total spin time. Strong dependence was observed for initial solute concentration and the final spin speed by Meyerhofer (17). Sukanek citesukanek85 proceeded further to consider the effects of evaporation rate on the spin speed and solute concentration. Jenekhe and Schuldt (10) extended this problem to the case of non-Newtonian fluid and studied the effects of elasticity on this flow. Lawrence (14) extensively reviewed some of the main contributions to the theory as well as experimental observations. But all these analyses were based on the typical hydro-dynamical approximation as employed by Emslie et al. (7).

Full Navier-Stokes equations were first considered by Higgins (8) to study the flow development through a matched asymptotic expansion procedure. Later, Dandapat and Ray (3; 4; 5) and Ray and Dandapat (19) extended the problem to study analytically the effects of thermocapillarity and magnetic field on the rate of film thinning. They observed that thermocapillary effect plays a vital role in enhancing the film thinning rate. In these studies it is tacitly assumed that the disk is wet so that the classical no-slip boundary condition can be applied at every point on the disk surface and the film flows under a planar interface for entire period of spinning. Another important class of problems viz. spreading of a liquid drop on a rotating disk in connection with the spin-coating is also studied by Troian et al. (21), Melo et al. (16), Moriarty et al. (18) and others. These studies were concerned with the motion of the contact line on the spinning disk and its stability. A recent study by Wilson et al. (23) of a spreading thin drop on a rotating disk shows that the profile of the spreading film becomes flat except near the contact line where capillary ridge forms that ultimately leads to the onset of instability.

To the best of our knowledge, only Matsumoto et al. (15), Wang et al. (24) and Kitamura (12) considered non-planar free surface and studied the unsteady problem. Matsumoto et al. (15) assumed a hemi-spherical liquid blob on the wetted surface of the disk and studied numerically spreading of the blob on a rotating surface and the role of different forces on the development of thin film. Using a similarity transformation on both time and space (radial coordinate  $r$ ), Wang et al. (24) reduced the Navier-Stokes equations to a set ordinary differential equations and solved these numerically. The present study is parallel to that of Kitamura (12) as both of these studies are on the unsteady development of

a thin film on a rotating disk for initial non-planar free surface. Kitamura (12) considered a hemi-spheroidal shaped liquid blob placed on the center of the disk and studied the evolution of film thickness on the surface using an expansion for the film thickness in powers of  $r^2$  and obtained the composite transient film thickness. Thus their solution is valid for small values of  $r$ , whereas our solution (see below) is valid at all values of  $r$  for thin films.

In this paper, we consider the spreading of a thin liquid film (with uniform non-uniform initial thickness) on an annular spinning disk which is initially wet. The chief justification for the use of this type of disk is that the liquid moves radially outward by the action of centrifugal force, and the flow eventually becomes uniform at a sufficient distance from the center of the disk. Therefore most the substrates get deposited in the grooves at a large  $r$  (say  $r > a$ ). In order to minimize the wastage of the expensive coating liquid which are used up for the formation of the thin film at  $r < a$ , this type of spinning disk is generally used for spin coating. We obtain asymptotic solution for the thickness of the thin film as a function of  $r$  using an expansion for the film thickness in powers of a small parameter characterizing the thickness of the film and applying the method of matched asymptotic expansion. This solution for small values of  $\epsilon$  is valid for all values of  $r$  and can be used to calculate the thickness of the film with good accuracy at any point on the disk. Other quantities of interest such as the velocity field and the rate at which the fluid is depleted from the disk during thinning process are calculated using this asymptotic solution. Effects of initial topography of the free surface, surface tension, Froude number, and Reynolds number are also addressed. We qualitatively and quantitatively predict various features of the thinning process which agree well with the existing numerical and experimental results.

## 2 GOVERNING EQUATIONS AND BOUNDARY CONDITIONS

We consider an axisymmetric flow of a thin film of an incompressible viscous liquid on a planar annular disk which rotates about the its axis  $z$  passing through its center 'O'. It has inner and outer radius of  $R_0$  and  $R$  respectively, and has  $Q_0$  amount of liquid deposited on its surface. Our aim is to analytically study the evolution of initial film thickness:  $h(r, t = 0) = \hat{\delta}(r)$ ,  $R_0 < r < R$ . The appropriate characteristic length scales along the radial ( $r$ ) and the vertical direction ( $z$ ) are  $R_0$  and  $H_0$  respectively where  $H_0$ , the maximum value of the initial film thickness, is much smaller than the inner radius  $R_0$  which in turn is much smaller than the outer radius  $R$  of the annular disk.

During the spin-off stage, the centrifugal force and the viscous shear across the film are of comparable magnitude. At this stage, the Reynolds number  $Re (= U_0 H_0 / \nu)$  is of order one and the balance of these forces defines a characteristic time scale  $t_c$

given by

$$t_c = \nu / (\Omega H_0)^2, \quad (1)$$

where  $\Omega$  and  $\nu$  are the uniform angular velocity of the disk and the kinematic viscosity of the fluid respectively. The velocity scale  $U_0$  is defined as  $(R_0 / t_c)$ . Using these scales we introduce the following dimensionless variables as

$$\begin{aligned} t' &= t_c \tau, \quad r' = R_0 r, \quad z' = H_0 z, \quad h' = H_0 h, \\ \hat{\delta}' &= H_0 \hat{\delta}, \quad u' = U_0 u, \\ v' &= (U_0 / \sqrt{\epsilon Re}) v, \quad w' = \epsilon U_0 w, \quad \text{and} \\ p' &= (\nu R_0^2 \rho / H_0^2 t_c) p, \end{aligned} \quad (2)$$

where the primed variables denote the relevant dimensional quantities and the dimensionless parameter  $\epsilon = H_0 / R_0$  is very small according to our previous assumptions. Using (2) in the equation of continuity and in Navier-Stokes equations reduce these to the following dimensionless form.

$$\left. \begin{aligned} u_r + (u/r) + w_z &= 0, \\ \epsilon Re [u_\tau + uu_r + ww_z] - (v^2/r) &= \\ -p_r + u_{zz} + \epsilon^2 [u_{rr} + (u/r)_r], \\ \epsilon Re [v_\tau + uv_r + (uv/r) + wv_z] &= \\ v_{zz} + \epsilon^2 [v_{rr} + (v/r)_r], \\ \epsilon^3 Re [w_\tau + uw_r + ww_z] &= \\ -p_z + \epsilon^2 w_{zz} + \epsilon^4 [w_{rr} + w_r/r] - \epsilon Re Fr^{-2}, \end{aligned} \right\} \quad (3)$$

where  $u(r, z, t)$ ,  $v(r, z, t)$ ,  $w(r, z, t)$  are the components of fluid velocities in the  $r$ ,  $\theta$  and  $z$  directions respectively,  $p$  is the pressure and the Froude number  $Fr = \sqrt{(\Omega^4 R_0^2 H_0^3 / g \nu^2)}$  in which  $g$  is the gravity. Here the subscripts denote differentiation with respect to the indicated variables. Following are the corresponding boundary and initial conditions in dimensionless form.

- *No-slip condition on the disk surface at  $z = 0$ :*

$$\begin{aligned} u(r, 0, \tau) &= 0, \quad v(r, 0, \tau) = r, \\ w(r, 0, \tau) &= 0. \end{aligned} \quad (4)$$

- *Shear stress vanishes along the interface at  $z = h(r, \tau)$ :*

$$\begin{aligned} 2\epsilon^2 h_r (w_z - u_r) + \\ (1 - \epsilon^2 h_r^2) (\epsilon^2 w_r + u_z) &= 0, \end{aligned} \quad (5)$$

$$v_z - \epsilon^2 r h_r (v/r)_r = 0. \quad (6)$$

- *Jump in the normal stress across the interface is balanced by the surface tension times curvature at  $z = h(r, \tau)$ :*

$$\begin{aligned}
& -p + 2\varepsilon^2(1 + \varepsilon^2 h_r^2)^{-1} \\
& [w_z - h_r u_z + \varepsilon^2(h_r^2 u_r - h_r w_r)] - \\
& \varepsilon^3 We [h_{rr}(1 + \varepsilon^2 h_r^2)^{-3/2} \\
& + (h_r/r)(1 + \varepsilon^2 h_r^2)^{-1/2}] = 0. \tag{7}
\end{aligned}$$

Here, the Weber number

$$We = (\sigma_0/R_0 H_0^2 \Omega^2 \rho)$$

in which  $\rho$  is the density and  $\sigma_0$  is the surface tension acting on the free surface of the fluid. In the analysis above, we have assumed  $Re Fr^{-2} = \overline{Fr}$  and  $\overline{We} = \varepsilon^2 We$ , where  $\overline{We} \sim O(1)$ . This implies that surface tension is large and is of the order  $O(\varepsilon^{-2})$ .

- *The kinematic condition at  $z = h(r, \tau)$ :*

$$h_\tau + u h_r = w. \tag{8}$$

In deriving the above free surface conditions, we have assumed that adjacent to the liquid film at the free surface is a gas or liquid vapor, and therefore the viscosity ratio  $\mu_g/\mu_l$ , where  $\mu_l$  and  $\mu_g$  are the viscosities of the liquid and gas phases respectively, is much less than unity and any motion of the gas is neglected. Further we assume that all physical properties viz. viscosity, surface tension etc. are constant in the subsequent analysis.

- *The initial conditions:*

$$\begin{aligned}
u(r, z, 0) &= v(r, z, 0) \\
&= w(r, z, 0) = 0, \quad z > 0, \\
h(r, 0) &= \delta(r), \\
1 &\leq r < R/R_0. \tag{9}
\end{aligned}$$

### 3 SOLUTION OF THE PROBLEM

For  $\varepsilon \ll 1$ , we look for asymptotic solution of the problem defined by (3)-(9) by expanding the dependent variables in powers of  $\varepsilon$ .

$$\begin{aligned}
F(r, z, \tau) &\sim F_0(r, z, \tau) \\
&+ \varepsilon F_1(r, z, \tau) + O(\varepsilon^2). \tag{10}
\end{aligned}$$

Using (10) in (3)-(7) and collecting the zeroth-order terms, we have

$$\left. \begin{aligned}
u_{0r} + (u_0/r) + w_{0z} &= 0, \\
u_{0zz} + v_0^2/r &= p_{0r}, \\
v_{0zz} &= 0, \\
p_{0z} &= 0.
\end{aligned} \right\} \tag{11}$$

The corresponding zeroth-order boundary conditions are

$$u_0 = w_0 = 0, \quad v_0 = r, \quad \text{at } z = 0 \tag{12}$$

$$u_{0z} = v_{0z} = 0, \quad p_0 = 0, \quad \text{at } z = h(r, \tau). \tag{13}$$

Without any loss of generality, we have taken in the above  $p_0 = 0$ . It is clear from the set of coupled equations (11) that the zeroth-order equations are independent of time. The solutions of the system (11) subject to the boundary conditions (12) and (13) are

$$u_0 = r(hz - \frac{z^2}{2}), \tag{14}$$

$$v_0 = r, \tag{15}$$

$$w_0 = \frac{1}{3}z^3 - hz^2 - \frac{1}{2}rz^2 h_r, \tag{16}$$

$$p_0 = 0. \tag{17}$$

Similarly, we obtain the following solutions of the first-order system of equations.

$$\left. \begin{aligned}
 u_1 &= -\overline{Fr} h_r + \overline{We} \left[ h_{rrr} + \frac{h_{rr}}{r} - \frac{h_r}{r^2} \right] \\
 &\quad \left[ hz - \frac{z^2}{2} \right] + Re \left[ rh_\tau \left( \frac{z^3}{6} - \frac{h^2 z}{2} \right) + \right. \\
 &\quad \left. + \frac{r^2 h h_r}{24} z^4 + \frac{2}{9} r h^3 z^3 - \frac{3}{5} r h^5 z \right. \\
 &\quad \left. - \frac{r^2 h^4 h_r}{6} z + \frac{r z^6}{360} - \frac{r h z^5}{60} \right], \\
 v_1 &= Re \left[ \frac{r h z^3}{3} - \frac{2}{3} r h^3 z - \frac{r}{12} z^4 \right], \\
 w_1 &= \frac{1}{r} \left[ \overline{We} \left\{ r \left[ \frac{1}{r} (r h_r)_r \right]_r \right\} \right. \\
 &\quad \left. - \overline{Fr} (r h_r)_r \right] \left( \frac{z^3}{6} - \frac{h z^2}{2} \right) \\
 &\quad + \left[ \overline{Fr} h_r - \overline{We} \left[ \frac{1}{r} (r h_r)_r \right]_r \right] \left( \frac{h_r z^2}{2} \right) \\
 &\quad + Re \left[ \frac{h z^6}{180} - \frac{z^7}{1260} - \frac{h^3 z^4}{9} + \frac{3 h^5}{5} z^2 \right. \\
 &\quad \left. + \frac{r h_r}{360} z^6 - \frac{r h h_r}{40} z^5 - \frac{r h^2 h_r}{6} z^4 \right. \\
 &\quad \left. + \frac{7}{4} r h^4 h_r z^2 - \frac{r^2 h_r^2}{120} z^5 + \frac{r^2 h^3 h_r^2}{3} z^2 \right. \\
 &\quad \left. - \frac{r^2 h h_{rr}}{120} z^5 + \frac{r^2 h^4 h_{rr}}{12} z^2 + \frac{h^2 h_\tau}{2} z^2 \right. \\
 &\quad \left. - \frac{h_\tau}{12} z^4 - \frac{r h_{r\tau}}{24} z^4 \right. \\
 &\quad \left. + \frac{r h^2 h_{r\tau}}{4} z^2 + \frac{r h h_r h_\tau}{2} z^2 \right].
 \end{aligned} \right\} \quad (18)$$

Thus the effect of the surface tension enters into this asymptotic solution at the first order through  $\overline{We}$ .

Using equations for  $u_1$  and  $w_1$  from (18) in the kinematic boundary condition (8) for  $u$  and  $w$  respectively, the long time

evolution equation for  $h$ , accurate up to  $O(\varepsilon)$ , becomes

$$\begin{aligned}
 h_\tau + \frac{1}{3r} \left( r^2 h^3 - \varepsilon \left\{ r h^3 \left[ \overline{Fr} h_r \right. \right. \right. \\
 \left. \left. - We \left( \frac{1}{r} [r h_r]_r \right) \right] \right. \\
 \left. + \frac{Re}{4} \left( \frac{5}{2} r^2 h^4 h_\tau + \frac{9}{10} r^3 h^6 h_r \right. \right. \\
 \left. \left. + \frac{311}{105} r^2 h^7 \right) \right\} \right) + O(\varepsilon^2) = 0, \quad (19)
 \end{aligned}$$

which exactly matches with the equation (5) of Kitamura (12). The present analysis deviates from that of Kitamura (12) in which an expansion of the film profile  $h(r, \tau)$  in powers of  $r^2$  is used to study the evolution of film thickness.. Thus his analysis is valid near the rotational axis (at  $r = 0$ ) only. For asymptotic solution for small values of  $\varepsilon$  which is valid for all values of  $r$ , we instead expand the film profile  $h(r, \tau)$  in powers of  $\varepsilon$

$$h(r, \tau) \sim h_0(r, \tau) + \varepsilon h_1(r, \tau) + O(\varepsilon^2). \quad (20)$$

Using (20) in (19) and collecting the coefficients of orders up to  $\varepsilon$ , we obtain at the lowest order the following governing equation

$$h_{0\tau} + r h_0^2 h_{0r} = -\frac{2}{3} h_0^3, \quad (21)$$

while at order  $\varepsilon$  we have

$$\begin{aligned}
 h_{1\tau} + r h_0^2 h_{1r} &= -2(h_0^2 + r h_0 h_{0r}) h_1 \\
 &+ \frac{1}{3r} \left[ r h_0^3 \left\{ \overline{Fr} h_{0r} - \overline{We} \left[ \frac{1}{r} (r h_{0r})_r \right]_r \right\} \right. \\
 &\left. + Re \left( \frac{34}{105} r^2 h_0^7 - \frac{2}{5} r^3 h_0^6 h_{0r} \right) \right]_r. \quad (22)
 \end{aligned}$$

It follows from equation (21) that

$$\frac{d}{d\tau} h_0(r(\tau), \tau) = -\frac{2}{3} h_0^3(r(\tau), \tau), \quad (23)$$

along the characteristic curve  $r(\tau)$  satisfying

$$\frac{d}{d\tau} r(\tau) = r(\tau) h_0^2(r(\tau), \tau). \quad (24)$$

Upon integration, these two equations give

$$\begin{aligned} h_0(r(\tau), \tau) &= c_0 \left(1 + \frac{4}{3} c_0^2 \tau\right)^{-\frac{1}{2}} \text{ along} \\ r(\tau) &= c_1 \left(1 + \frac{4}{3} c_0^2 \tau\right)^{\frac{3}{4}}. \end{aligned} \quad (25)$$

It also follows from (25) that along each characteristic curve (24),

$$r(\tau) h_0^{\frac{3}{2}}(r(\tau), \tau) = c_1 c_0^{2/3} = \text{constant}. \quad (26)$$

Here  $c_0$  and  $c_1$  are characteristic-curve-dependent constants. Since the above equations are valid at large times, these constants  $c_0$  and  $c_1$  can be related to initial data by matching these solutions with small time solutions which we discuss later in the next section. These two equations in (25) can be combined to obtain

$$r(\tau) = c_1 h_0^{-\frac{3}{2}}(r(\tau), \tau) \left( \frac{1}{h_0^2(r(\tau), \tau)} - \frac{4}{3} \tau \right)^{-\frac{3}{4}}, \quad (27)$$

which is in agreement with the works of Melo et al. (16) and Moriarty et al. (18) on the spreading of a drop on a rotating disk.

Similarly, it follows from equation (22) that  $h_1$  can be integrated along the same characteristic curve (24). In so doing, we obtain

$$\begin{aligned} h_1(r(\tau), \tau) &= -\frac{2}{9\overline{Fr}} c_0^2 c_1^{-2} \chi^{-5/2} \\ &+ \frac{32}{81\overline{We}} c_0^2 c_1^{-4} \chi^{-4} \\ &+ \frac{62}{315} Re c_0^5 \chi^{-\frac{5}{2}} + c_2 \chi^{-\frac{1}{2}}, \end{aligned} \quad (28)$$

along the characteristic curve (24). In the above,  $\chi = (1 + 4c_0^2\tau/3)$  and  $c_2$  is the constant of integration. In order to find the constants  $c_0, c_1, c_2$  by matching these solutions with short time solutions, we next find short time solutions.

### 3.1 Short time analysis

At the spun-up stage, the time scale is dictated by the fact that the local inertial term is of the same order of magnitude as the viscous and the centrifugal terms in the governing equations. The appropriate time scale is then given by

$$\begin{aligned} t &= \tau/\varepsilon, \quad \bar{u} = u, \quad \bar{v} = v, \quad \bar{w} = w, \\ \bar{h} &= h, \quad \bar{p} = p, \quad \bar{r} = r, \quad \text{and} \quad \eta = z, \end{aligned} \quad (29)$$

where new notations are introduced for short-time solutions for all other variable. In these variables, the governing equations of motion become

$$\left. \begin{aligned} \bar{u}_{\bar{r}} + (\bar{u}/\bar{r}) + \bar{w}_{\eta} &= 0, \\ Re \bar{u}_t + \varepsilon Re [\bar{u} \bar{u}_{\bar{r}} + \bar{w} \bar{u}_{\eta}] \\ &- (\bar{v}^2/\bar{r}) = -\bar{p}_{\bar{r}} + \bar{u}_{\eta\eta} \\ &+ \varepsilon^2 [\bar{u}_{\bar{r}\bar{r}} + (\bar{u}/\bar{r})_{\bar{r}}], \\ Re \bar{v}_t + \varepsilon Re [\bar{u} \bar{v}_{\bar{r}} + (\bar{u}\bar{v}/\bar{r}) + \bar{w} \bar{v}_{\eta}] &= \\ \bar{v}_{\eta\eta} + \varepsilon^2 [\bar{v}_{\bar{r}\bar{r}} + (\bar{v}/\bar{r})_{\bar{r}}], \\ \varepsilon^2 Re \bar{w}_t + \varepsilon^3 Re [\bar{u}\bar{w}_{\bar{r}} + \bar{w}\bar{w}_{\eta}] &= \\ -\bar{p}_{\eta} + \varepsilon^2 [\varepsilon^2 \bar{w}_{\bar{r}\bar{r}} + \frac{\varepsilon^2}{\bar{r}} (\bar{w}_{\bar{r}}) \\ &+ \bar{w}_{\eta\eta}] - \varepsilon \overline{Fr}. \end{aligned} \right\} \quad (30)$$

The associated boundary conditions reduce to

$$\bar{u} = \bar{w} = 0, \quad \bar{v} = \bar{r} \quad \text{at} \quad \eta = 0, \quad (31)$$

$$\left. \begin{aligned} 2\varepsilon^2 \bar{h}_{\bar{r}} (\bar{w}_{\eta} - \bar{u}_{\bar{r}}) + \\ (1 - \varepsilon^2 \bar{h}_{\bar{r}}^2) (\varepsilon^2 \bar{w}_{\bar{r}} + \bar{u}_{\eta}) &= 0, \\ \bar{v}_{\eta} - \varepsilon^2 \bar{r} \bar{h}_{\bar{r}} (\bar{v}/\bar{r})_{\bar{r}} &= 0, \\ -\bar{p} + 2\varepsilon^2 (1 + \varepsilon^2 \bar{h}_{\bar{r}}^2)^{-1} \\ [\bar{w}_{\eta} + \varepsilon^2 \bar{u}_{\bar{r}} \bar{h}_{\bar{r}}^2 - \varepsilon^2 \bar{w}_{\bar{r}} \bar{h}_{\bar{r}} - \bar{u}_{\eta} \bar{h}_{\bar{r}}] \\ - \varepsilon^3 c^{-1} [\bar{h}_{\bar{r}\bar{r}} (1 + \varepsilon^2 \bar{h}_{\bar{r}}^2)^{3/2} \\ + (1 + \varepsilon^2 \bar{h}_{\bar{r}}^2)^{-1/2} (\bar{h}_{\bar{r}}/\bar{r})] &= 0, \end{aligned} \right\} \quad (32)$$

$$\text{at} \quad \eta = \bar{h}, \quad (32)$$

$$\bar{h}_t + \varepsilon \bar{u} \bar{h}_{\bar{r}} = \varepsilon \bar{w} \quad \text{at} \quad \eta = \bar{h}, \quad (33)$$

and the initial conditions remain the same, i.e.

$$\begin{aligned} \bar{u}(\bar{r}, \eta, 0) = \bar{w}(\bar{r}, \eta, 0) = \bar{v}(\bar{r}, \eta, 0) &= 0, \\ \bar{h}(\bar{r}, 0) &= \delta(\bar{r}), \end{aligned} \quad (34)$$

for all values of  $z$  and  $r$  in the film. The matching conditions are derived from the requirement that, for continuity in the flow structure, the flows in the spin-off and the spun-up stages are smoothly connected. This leads to the condition

$$\lim_{t \rightarrow \infty} F_{SU} = \lim_{\tau \rightarrow 0} F_{SO}, \quad (35)$$

where the subscripts ‘ $SU$ ’ and ‘ $SO$ ’ represent the spun-up (short time) and spin-off (long time) stages respectively. Expanding the variables in powers of  $\varepsilon$  (see (10)) and substituting these in (30)–(34), we obtain, to the leading-order, the following equations

$$\left. \begin{aligned} \bar{u}_{0\bar{r}} + (\bar{u}_0/\bar{r}) + \bar{w}_{0\eta} &= 0, \\ Re \bar{u}_{0t} - (\bar{v}_0^2/\bar{r}) &= -\bar{p}_{0\bar{r}} + \bar{u}_{0\eta\eta}, \\ Re \bar{v}_{0t} &= \bar{v}_{0\eta\eta}, \\ \bar{p}_{0\eta} &= 0, \end{aligned} \right\} \quad (36)$$

with the boundary conditions

$$\begin{aligned}\bar{u}_0(\bar{r}, 0, t) = \bar{w}_0(\bar{r}, 0, t) = 0, \\ \bar{v}_0(\bar{r}, 0, t) = \bar{r},\end{aligned}\quad (37)$$

$$\begin{aligned}\bar{u}_{0\eta} = \bar{v}_{0\eta} = 0, \quad \bar{p}_0 = 0, \text{ on} \\ \eta = \bar{h}(\bar{r}, t),\end{aligned}\quad (38)$$

$$\bar{h}_{0t} = 0, \text{ on } \eta = \bar{h}(\bar{r}, t),\quad (39)$$

and the initial conditions as

$$\begin{aligned}\bar{u}_0(\bar{r}, \eta, 0) = \bar{w}_0(\bar{r}, \eta, 0) \\ = \bar{v}_0(\bar{r}, \eta, 0) = 0,\end{aligned}\quad (40)$$

$$\bar{h}_0(\bar{r}, 0) = \delta(\bar{r}).\quad (41)$$

From (39) and (41), we have

$$\begin{aligned}\bar{h}_0(\bar{r}, t) = \delta(\bar{r}), \quad \text{for } t \geq 0, \\ 1 \leq \bar{r} < R/R_0.\end{aligned}\quad (42)$$

The solutions of equations in (36) satisfying (37)–(38) and (40) are

$$\begin{aligned}\bar{u}_0(\bar{r}, \alpha, t) = \bar{r} \left[ \delta^2(\bar{r}) \left( \alpha - \frac{\alpha^2}{2} \right) \right. \\ \left. - 2\delta^2(\bar{r}) \sum_{p=1(2)}^{\infty} \frac{\sin(\lambda_p \alpha)}{\lambda_p^3} \right. \\ \left. \exp(-\lambda_p^2 t / Re \delta^2(\bar{r})) \right. \\ \left. - \frac{4t}{Re} \sum_{p=1(2)}^{\infty} \frac{(\sin \lambda_p \alpha)}{\lambda_p} \right. \\ \left. \exp(-\lambda_p^2 t / Re \delta^2(\bar{r})) \right. \\ \left. - 16 \sum_{p=1(2)}^{\infty} \sum_{n=1(2)}^{\infty} \frac{\delta^2(\bar{r}) A_{np}^o}{(\lambda_p^2 - 2\lambda_n^2)} \right.\end{aligned}$$

$$\begin{aligned}\times (\sin(\lambda_p \alpha) \{ \exp(-\lambda_n^2 t / Re \delta^2(\bar{r})) \\ - \exp(-\lambda_p^2 t / Re \delta^2(\bar{r})) \}) \\ - 32 \sum_{p=1(2)}^{\infty} \sum_{n=1(2)}^{\infty} \sum_{l>n}^{\infty} \\ \frac{\delta^2(\bar{r}) A_{np}^l}{\lambda_p^2 - (\lambda_n^2 + \lambda_l^2)} \\ \times \sin(\lambda_p \alpha) \{ \exp(-(\lambda_n^2 + \lambda_l^2) t / Re \delta^2(\bar{r})) \\ - \exp(-\lambda_p^2 t / Re \delta^2(\bar{r})) \} \Big],\end{aligned}$$

$$\bar{v}_0(\bar{r}, \alpha, t) = \bar{r} \left[ 1 - 2 \sum_{n=1(2)}^{\infty} \frac{\sin(\lambda_n \alpha)}{\lambda_n} \right. \\ \left. \exp(-\lambda_n^2 t / Re \delta^2(\bar{r})) \right],$$

$$\begin{aligned}\bar{w}_0(\alpha, t) = \delta^3(\bar{r}) \left( \frac{\alpha^3}{3} - \alpha^2 \right) \\ - 4\delta^3(\bar{r}) \sum_{p=1(2)}^{\infty} \frac{\cos(\lambda_p \alpha) - 1}{\lambda_p^4} \\ \exp(-\lambda_p^2 t / Re \delta^2(\bar{r})) \\ - \frac{8t\delta(\bar{r})}{Re} \sum_{p=1(2)}^{\infty} \frac{\cos(\lambda_p \alpha) - 1}{\lambda_p^2} \\ \exp(-\lambda_p^2 t / Re \delta^2(\bar{r})) - 32\delta^3(\bar{r}) \sum_{p=1(2)}^{\infty} \\ \sum_{n=1(2)}^{\infty} \frac{A_{np}^o}{\lambda_p(\lambda_p^2 - 2\lambda_n^2)} \\ \times (\cos(\lambda_p \alpha) - 1) \{ \exp(-2\lambda_n^2 t / Re \delta^2(\bar{r})) \\ - \exp(-2\lambda_p^2 t / Re \delta^2(\bar{r})) \} \\ - 64\delta^3(\bar{r}) \sum_{p=1(2)}^{\infty} \sum_{n=1(2)}^{\infty} \sum_{l>n}^{\infty} \\ \frac{A_{np}^l \{ \cos(\lambda_p \alpha) - 1 \}}{\lambda_p \{ \lambda_p^2 - \lambda_n^2 - \lambda_l^2 \}} \\ \times \{ \exp[-(\lambda_n^2 + \lambda_l^2) t / Re \delta^2(\bar{r})] \\ - \exp[-\lambda_p^2 t / Re \delta^2(\bar{r})] \},\end{aligned}\quad (43)$$

where  $\eta = \alpha\delta(\bar{r})$ ,  $\lambda_n = n\pi/2$ ,  $n = 1, 3, 5, \dots$ ,  $A_{np}^o = 1/(\lambda_p(\lambda_p^2 - 4\lambda_n^2))$  and  $A_{np}^l = \lambda_p/(\lambda_p^4 + (\lambda_n^2 - \lambda_l^2)^2 - 2\lambda_p^2(\lambda_n^2 + \lambda_l^2))$ . Since the free surface will vary within  $0 \leq \eta \leq \delta(\bar{r}) \leq 1$  after the start of the rotation of the disk, we have assumed that  $0 \leq \alpha \leq 1$  in finding (42). To complete the solution we need to calculate the first-order correction to the film thickness for short time. From

the kinematic condition we obtain the first-order correction as

$$\begin{aligned}
\bar{h}_1(\bar{r}, t) = & -\frac{2}{3}\delta^3(\bar{r})t - 4\delta^5(\bar{r})Re \\
& \sum_{p=1(2)}^{\infty} \left( \frac{\exp(-\lambda_p^2 t / Re\delta^2(\bar{r})) - 1}{\lambda_p^6} \right) \\
& - \frac{8}{Re} \sum_{p=1(2)}^{\infty} \frac{1}{\lambda_p^2} \\
& \times \left\{ \frac{Re\delta^3(\bar{r})t}{\lambda_p^2} \exp[-\lambda_p^2 t / Re\delta^2(\bar{r})] \right. \\
& \left. + \frac{Re^2\delta^5(\bar{r})}{\lambda_p^4} (\exp[-\lambda_p^2 t / Re\delta^2(\bar{r})] - 1) \right\} \\
& - 32\delta^5(\bar{r})Re \sum_{p=1(2)}^{\infty} \sum_{n=1(2)}^{\infty} \frac{A_{np}^o}{\lambda_p(\lambda_p^2 - 2\lambda_n^2)} \\
& \times \left\{ \frac{\exp(-2\lambda_n^2 t / Re\delta^2(\bar{r})) - 1}{2\lambda_n^2} \right. \\
& \left. - \frac{\exp(-\lambda_p^2 t / Re\delta^2(\bar{r})) - 1}{\lambda_p^2} \right\} \\
& - 64\delta^5(\bar{r})Re \sum_{p=1(2)}^{\infty} \sum_{n=1(2)}^{\infty} \sum_{l>n}^{\infty} \\
& \frac{A_{np}^l}{\lambda_p \{ \lambda_p^2 - (\lambda_n^2 + \lambda_l^2) \}} \\
& \times \left\{ \frac{\exp(-(\lambda_n^2 + \lambda_l^2)t / Re\delta^2(\bar{r})) - 1}{(\lambda_n^2 + \lambda_l^2)} \right. \\
& \left. - \frac{\exp(-\lambda_p^2 t / Re\delta^2(\bar{r})) - 1}{\lambda_p^2} \right\}, \quad (44)
\end{aligned}$$

where  $\bar{h}_1(\bar{r}, 0) = 0$  is used. Comparing the above equation (44) with equations (8a) and (8b) of Kitamura (12), one can see that the terms for gravity and surface tension are absent from (44). This is due to the fact that the contributions of these terms in short time analysis are of the order  $O(\epsilon^2)$  and we have considered only up to  $O(\epsilon)$ . But the effects of these terms become prominent at large times (see equations (18) and (22)).

### 3.2 Matched asymptotic solution

First we calculate  $c_0$  and  $c_1$  associated with equations in (25) by using the condition (35) on  $h_0$ , i.e.

$$\lim_{t \rightarrow \infty} \bar{h}_0(t) = \lim_{\tau \rightarrow 0} h_0(\tau). \quad (45)$$

Since the solution  $\bar{h}_0(\bar{r}, t)$  given by (42) does not depend on time  $t$ , the above matching condition implies that the solution (25) can

be applied up to  $\tau = 0$ , and this leads to

$$c_1 = r(0) = \xi \text{ (say)}, \quad c_0 = h_0(\xi, 0) = \delta(\xi). \quad (46)$$

Therefore, to find  $h_0(r, \tau)$ , one solves the equation (second equation in (25))

$$r(\tau) = \xi \left( 1 + \frac{4}{3}\tau\delta^2(\xi) \right)^{\frac{3}{4}} \quad (47)$$

for  $\xi$  and then (first equation in (25)) uses

$$h_0(r, \tau) = \delta(\xi) \left( 1 + \frac{4}{3}\tau\delta^2(\xi) \right)^{-\frac{1}{2}}. \quad (48)$$

However, the equation (47) may not have a unique solution because characteristics (47) may cross depending on the initial film thickness  $\delta(\xi)$ . If  $\tau_b$  denotes the first time when this happens, then we can find this by setting  $\frac{dr}{d\xi} = 0$ . A simple calculation shows that

$$\tau_b = \frac{-1}{\min \left[ \frac{4}{3}\delta^2(\xi) + 2\xi\delta(\xi)\delta'(\xi) \right]}. \quad (49)$$

Thus, the thin film which evolves in the form of a wave as it propagates outward first breaks at  $\tau = \tau_b$  just as a wave does on a beach. Later we will show such wave breaking phenomenon in the thin film evolution.

In order to find the first order correction to the film thickness, we first need to find the constant  $c_2$  that appear in (28). The constant  $c_2$  in (28) can also be estimated through the matching relation (35) between (28) and (44), and this gives

$$\begin{aligned}
& -\frac{2}{9}\overline{Fr} \delta^2(\xi)\xi^{-2} + \frac{32}{81}\overline{We} \delta^2\xi^{-4} \\
& + \frac{62}{315}Re \delta^5(\xi) + c_2 = 0.66087Re\delta^5(\xi). \quad (50)
\end{aligned}$$



Thus we obtain  $h_1(r, \tau)$  as

$$\begin{aligned}
h_1(r, \tau) &= \frac{32}{81} \overline{We} \delta^2(\xi) \xi^{-4} \left(1 + \frac{4}{3} \delta^2(\xi) \tau\right)^{-4} \\
&+ \left(\frac{62}{315} Re \delta^5(\xi) - \frac{2}{9} \overline{Fr} \delta^2(\xi) \xi^{-2}\right) \\
&\left(1 + \frac{4}{3} \delta^2(\xi) \tau\right)^{-5/2} \\
&+ \left(\frac{2}{9} \overline{Fr} \delta^2(\xi) \xi^{-2} + 0.46373 Re \delta^5(\xi)\right) \\
&- \frac{32}{81} \overline{We} \delta^2(\xi) \xi^{-4} \left(1 + \frac{4}{3} \delta^2(\xi) \tau\right)^{-1/2}. \quad (51)
\end{aligned}$$

As before, to find  $h_1(r, \tau)$  using the above formula, one first solves the equation (47) for  $\xi$  and then uses (52).

The composite uniform expansion (see Van Dyke (22)) for the transient film thickness  $h^c(r, t)$  is then given by

$$\begin{aligned}
h^c(r, \tau) &= [h_0(r, \tau) + \bar{h}_0(r, \tau/\varepsilon) - \delta(\xi)] \\
&+ \frac{2}{3} \delta^3(\xi) \tau + \varepsilon [h_1(r, \tau) \\
&+ \bar{h}_1(r, \tau/\varepsilon) - 0.66087 Re \delta^5(\xi)]. \quad (53)
\end{aligned}$$

To find the composite film thickness  $h^c(r, \tau)$ , one first solves the equation (47) to find  $\xi$ , and then finds  $h_0(r, \tau)$ ,  $\bar{h}_0(r, \tau/\varepsilon)$ ,  $h_1(r, \tau)$ ,  $\bar{h}_1(r, \tau/\varepsilon)$  using (48), (42), (52), (44) respectively, and finally the composite film thickness using (53).

#### 4 RESULTS AND DISCUSSION

Here we exemplify some of the phenomenon by considering the following initial film distribution  $h(r, 0) = \delta(r)$ .

$$\delta(r) = (r-1)e^{(2-r)}, \quad r \geq 1. \quad (54)$$

Figure 1 shows the variation of the film thickness  $h^c(r, \tau)$  with  $r$  at several values of time  $\tau$  for  $Fr = 0$  but for finite values of  $We$  and  $Re$ . It shows that the initial film thickness is larger in the central region than elsewhere. As the free surface of this film evolves, a wave-like front develops which migrates radially outward and the film behind this front gradually gets thinner with increasing time. Moreover, this wave as it propagates eventually breaks and the film height becomes triple-valued immediately afterward as seen in the plot for  $\tau = 1.5$  in this figure. This figure shows that the wave breaks at a time  $t : 0.5 < t < 1.5$  at  $\xi : 3.0 <$

$\xi < 5.0$ . A simple calculation involving (49) and (54) shows that this wave breaks for our example at  $\tau = \tau_b$  given by

$$\begin{aligned}
\tau_b &= \min \left\{ \frac{3e^{-2(2-\xi)}}{2(\xi-1)(3\xi^2-8\xi+2)} \right\} \\
&= 1.0553694 \quad \text{at } \xi = 3.21525. \quad (55)
\end{aligned}$$

This is consistent with the plots shown in Fig. 1. It is worth noting from our expressions for the wave breaking time and its location that surface tension, gravity and viscosity have no effect either on the wave breaking time or its location. However, the wave height at the time it breaks is somewhat mitigated by the surface tension due to its film-thinning effect (see below).

It is worth making some remarks about the effects of surface tension (Weber number), gravity (Froude number), and viscosity (Reynolds number) on the thinning process of the film. We notice from above that the Weber number, Froude number, and Reynolds number enter into the expression for the composite thickness  $h_c$  through  $h_1(r, \tau)$ . A simple manipulation of (52) with the help of (27) and (46) gives

$$\begin{aligned}
h_1(r, \tau) &= \frac{2}{9} \overline{Fr} h_0^2 r^{-2} (\chi^2 - 1) \\
&+ \frac{32}{81} \overline{We} r^{-4} h_0^2 (1 - \chi^{7/2}) \\
&+ Re h_0^5 \left( \frac{62}{315} + 0.46373 \chi^2 \right), \quad (56)
\end{aligned}$$

where  $\chi = (1 + 4\delta^2(\xi)\tau/3)$ .

This equation shows that the term which represents the effect of surface tension (through  $\overline{We}$ ) is negative. This implies that surface tension helps the thinning process of the film. It is also clear from (56) that the effect of surface tension is more important near  $r = 1$  and negligible for large  $r$ . As a result, the central region thins faster than the outer region. This is contrary to what one expects in the case of spreading of a drop under centrifugal force, where surface tension inhibits the spreading process of the drop. Both of these opposing effects of surface tension can be understood from the fact that the surface tension tends to minimize the surface area. In our case, the surface tension does so by helping the thinning process which reduces the surface area since the entire surface is wet to being with. In the case of a spreading drop, the surface area increases with drop spreading due to centrifugal force which is against what surface tension would like to do. Hence, in this case it opposes the spreading effect. Further, it can be seen from equation (56) that the gravity (through  $Fr$ ) and viscosity (through  $Re$ ) do not help the thinning process. However, it is seen from (56) that the effect of gravity is mild at large  $r \gg 1$ .

We have also investigated the effects of the initial amount of liquid deposited on the disk and the initial topography of the free-surface on the large time behavior of the thickness of the film. Results of a prototypical study of the effect of the initial topography of the free-surface with the operating time and the initial amount of fluid deposited remaining same are tabulated. Table I shows the film thickness for four values of  $r$  at  $\tau = 10$  and  $\tau = 20$  for two types of initial topography of the free surface: (i) planar with uniform film thickness; and (ii) non-planar with non-uniform distribution of initial film thickness given by (54). In both cases, same amount of fluid  $Q_0$  is deposited initially on the disk.

We find that the film thickness vary along the radial direction  $r$  during the evolution of the film from some initial data, even when the film is uniform initially. The free surface of the film in both cases (uniform and non-uniform initial thickness) becomes almost planar (except for a very small region near the inner perimeter) with uniform thickness at a later stage. For obvious reasons, this happens sooner when the film is initially uniform (see Table I). At this stage, the film for the case of non-uniform initial distribution is thinner as expected. However, the thinning process of the film continues beyond this stage and eventually the film attains an almost uniform thickness (for most part of the disk away from the central region) that is independent of the initial distributions considered. It is worth noting in Fig. 1 that the film becomes fairly of uniform height after  $r > 4$  at  $\tau = 20$  when all the wave breaking and thinning process have subsided. At very large times, we have obtained almost uniform film thickness of  $O(10^{-4})$  for  $r > 4$  for both types of initial topography of free surface.

Figure 2 shows variation of the film height with  $r$  at four different time levels  $\tau = 0.0, 2.0, 20.0, 500.0$  for uniform initial distributions ( $a$ ) and ( $a_1$ ) such that the amount of liquid in ( $a$ ) is more than that in ( $a_1$ ). It is clear from this figure that the final film thickness does not depend on the amount of liquid initially distributed. These above two results are consistent with the experimental findings of Daughton and Givens (6).

Next we show some plots of the velocity components of the fluid on the free surface. The plot of  $v$  versus  $r$  (which is not shown here) is linear as expected on the free surface due to no-slip condition. Figure 3 shows the plots of  $u$  and  $w$  against  $r$  for different values of  $\tau$ . It is worth mentioning here that the variation of  $v$  with  $\tau$  for fixed  $r$  is negligible.

$d\bar{Q}/d\tau$ , the rate at which the liquid is depleted from the disk, is shown against time  $\tau$  in Fig. 4 for both uniform and non-uniform (given by (54)) initial distributions. Here  $\bar{Q}$  is the amount of liquid depleted in time  $t$  and the initial amount of fluid  $Q_0$  are the same in both cases. It shows that most of the liquid flows out of the disk initially in a very short time. Thereafter,  $d\bar{Q}/d\tau$  decreases gradually with increasing time and attains the same value at  $\tau = 25$  for both uniform and non-uniform initial distributions. This means that rate at which the film thins de-

creases gradually and the thinning rate for both becomes same at  $\tau = 25$ . However, thinning rate eventually become zero at very large time which is not shown in this picture. The negative part of  $d\bar{Q}/d\tau$  in Fig. 4 for non-uniform initial distribution in fact represents the amount of liquid flowing in, and is more than that of the liquid flowing out of the annular disk. This figure also suggests that the rate of depletion at early stages of development is more for uniform initial distribution than the non-uniform one. In other words, the retention of fluid for non-uniform initial distribution is more than that for uniform distribution at early stages of the spreading of the thin film. This result is in excellent agreement with the findings of Hwang and Ma (9).

## 5 CONCLUSION

The asymptotic solution presented here provides some understanding of the film-thinning process associated with spin-coating. Some of our results explain experimentally observed facts and some provides new insights into the spin-coating process.

We find that the final thickness of the almost planar thin-film of uniform thickness does not depend on the initial topography (planar or non-planar) of the free surface and on the initial amount of liquid deposited on the spinning disk. For the same amount of liquid deposited initially, the non-planar initial free surface enhances film thinning when compared with planar free-surface. The surface tension is found to enhance film thinning, and hence attenuates the wave breaking phenomena to the extent that wave height is less severe when it breaks. However, the wave breaking time and its location where the wave breaks are not affected by any of the physical factors: surface tension, gravity or viscosity. However, this conclusion is based on  $O(\epsilon)$  accurate asymptotic solutions.

## ACKNOWLEDGMENT

It is a pleasure to thank Texas A&M University and ISI, Calcutta, India for providing resources for the completion of this work.

## REFERENCES

- Drazin, P. G., and Reid, W. H. Reid, 1982, *Hydrodynamic Stability*, Cambridge, New York.
- Evans, D. V., 1968, "The effect of surface tension on the waves produced by a heaving circular cylinder," *Proc. Camb. Phil. Soc.*, **64**, pp. 833-847.
- Dandapat, B. S., and Ray, P. C., 1990, "Film cooling on a rotating disk," *Int. J. Non-Linear Mech.*, **25**, pp. 569-582.
- Dandapat, B. S., and P.C. Ray, 1994, "The effect of thermocapillarity on the flow of a thin liquid film on a rotating disk," *J. Phys. D: Appl. Phys.*, **27**, pp. 2041-2045.

Dandapat, B. S., and Ray, P. C., 1998, "Effect of thermocapilarity on the production of a conducting thin film in presence of a transverse magnetic field," *ZAMM*, **78**, pp. 635-640.

Daughton, W. J., and Givens, F. L., 1982, "An investigation of the thickness variation of spun-on thin films commonly associated with the semiconductor industry," *J. Electrochem. Soc.*, **129**, pp. 173-179.

Emslie, A. C., F. D. Bonner, and L. G. Peck, 1958, "Flow of a viscous liquid on a rotating disk," *J. Appl. Phys.*, **29**, pp. 858-862.

Higgins, B. G., (1986), "The effect of inertia and interfacial shear on film flow on a rotating disk," *Phys. Fluids*, **29**, pp. 3522-3529.

Hwang, J. H., and Ma, F., 1989, "On the flow of a thin liquid film over a rough rotating disk," *J. Appl. Phys.*, **66**, pp. 388-394.

Jenekhe, S. A., and Schuldt, S. A., 1984, "Coating flow of non-Newtonian fluids on a flat rotating disk," *Ind. Engg. Chem. Fundam.*, **23**, pp. 432-436.

Kapitza, P. L., 1948, "Wave flow of thin viscous fluid layers," *zh. Eksp. Tero. Fiz.*, **18**, pp. 3-28.

Kitamura, A., 2000, "Asymptotic solution for film flow on a rotating disk," *Phys. Fluids*, **12**, pp. 2141-2144.

Larson, R. G., and Rehg, T. G., 1997, "Spin Coating," In *Liquid Film Coating*, S. K. Kistler et al., eds., Chapman Hall, London, pp. 709-734.

Lawrence, C. J., 1988, "The mechanics of spin coating of polymer films," *Phys. Fluids*, **31**, pp. 2786-2795.

Matsumoto, Y., Ohara, T., Teruya, T., and Ohashi, H., 1989, "Liquid film formation on a rotating disk," *JSME Int. J., Ser.II*, **32**, pp. 52-56.

Melo, F., Joanny, J. F., and Fauve, S., 1989, "Fingering instability of spinning drops," *Phys. Rev. Lett.*, **63**, pp. 1958-1961.

Meyerhofer, D., 1978, "Characteristics of resist films produced by spinning," *J. Appl. Phys.*, **47**, pp. 3993-3997.

Moriarty, J. A., Schwartz, L. W., and Tuck, E. O., 1991, "Unsteady spreading of thin liquid films with small surface tension," *Phys. Fluids*, **3**, pp. 733-742.

Ray, P. C., and Dandapat, B. S., 1992, "Flow of thin liquid film on a rotating disk in presence of a transverse magnetic field," *Quart. J. Mech. Appl. Math.*, **47**, pp. 297-304.

Sukanek, P. C., 1985, "Spin coating," *J. Imaging Technol.*, **11**, pp. 184-191.

Troian, S. M., Herbolzheimer, E., Safran, S. A., and Joanny, J. F., 1989, "Fingering instabilities of driven spreading films," *Europjysics Lett.*, **63**, pp. 25-30.

Van Dyke, M., 1964, *Perturbation Methods in Fluid Mechanics*, Academic Press, New York.

Wilson, S. K., 2000, "The rate of spreading in spin coating," *J. Fluid Mech.*, **413**, pp. 65-88.

Wang, C. Y., Watson, L. T., and Alexander, K. A., 1991, "Spinning of a liquid film from an accelerating disk," *IMA J. Appl. Math.*, **46**, pp. 201-210.

Table 1. Comparison of the film thickness  $h^c(r, \tau)$  at several values of  $r$  and  $\tau$ , when same amount of fluid  $Q_0$  is distributed initially either as a uniform or non-uniform distribution

$r$	$\tau = 10.00$	
	uniform film distribution	non-uniform film distribution
1.2	0.243	0.112
3.2	0.244	0.234
4.2	0.244	0.250
5.2	0.244	0.253

$r$	$\tau = 20.00$	
	uniform film distribution	non-uniform film distribution
1.2	0.181	0.082
3.2	0.183	0.167
4.2	0.183	0.176
5.2	0.183	0.180

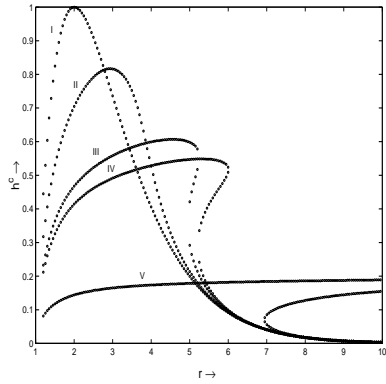


Figure 1. Variation of the film thickness  $h^c(r, \tau)$  for non-uniform initial distribution with respect to  $r$  for several values of time  $\tau$ :  $\tau = 0.0$  (I),  $\tau = 0.5$  (II),  $\tau = 1.5$  (III),  $\tau = 2.0$  (IV),  $\tau = 20.0$  (V).

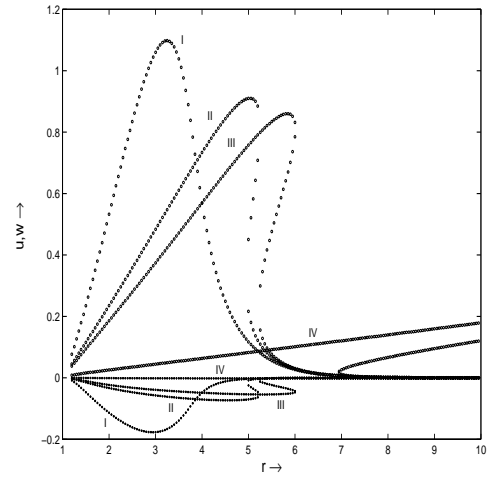


Figure 3. Variation of  $u$  and  $w$  with respect to several values of  $\tau$ : 'I' represents for  $\tau = 0.5$ , 'II' for  $\tau = 1.5$ , 'III' for  $\tau = 2.0$ , and 'IV' for  $\tau = 20.0$ . (for non-uniform initial distribution).

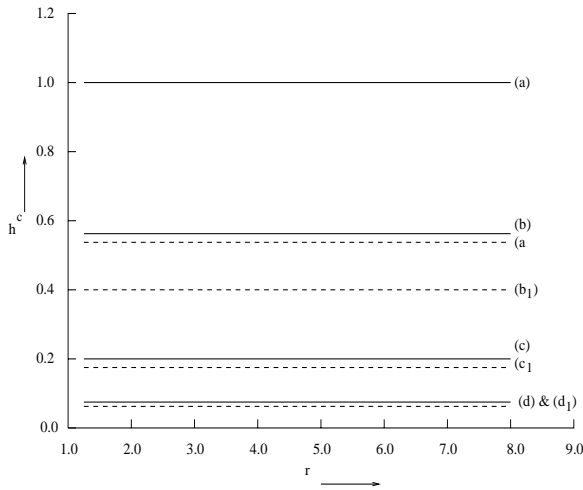


Figure 2. Variation of the film height  $h^c(r, \tau)$  for initial distribution having different amount of initial liquid deposition  $Q_1$  and  $Q_2$  such that  $Q_1 > Q_2$  with respect to  $r$  for several values of time  $\tau$ . Solid line represents the subsequent developments of the amount  $Q_1$  and the dotted line for  $Q_2$ . (a) and (a<sub>1</sub>) represents for time  $\tau = 0.0$ , (b) and (b<sub>1</sub>) for  $\tau = 2.0$  while (c) and (c<sub>1</sub>) for  $\tau = 20.0$  and (d) and (d<sub>1</sub>) for  $\tau = 500.00$ .

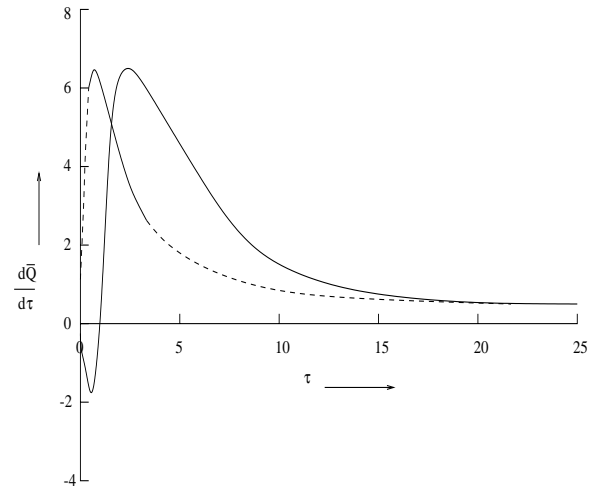


Figure 4. Variation of the rate at which the amount of liquid is depleted from the disk with time for both uniform (dotted line) and non-uniform (solid line) initial distributions.